

Supplementary Information

Contents

Appendix S1. Methods for reconstruction of <i>DBH</i>	2
Appendix S2. Methods for comparing climwin results with traditional methods	3
Appendix S3. Dealing with rapidly changing climate and tree growth	4
Table S1. Site Details	5
Table S2. Species analyzed, their characteristics, and bark allometries applied	6
Table S3. Sampling details for species by site	7
Table S4. Allometric equations for bark thickness	8
Table S5. Qualitative comparison of results from this study with previous studies employing conventional methods	9
Table S6. Frequency of <i>DBH</i> -climate interactions across all sites and growth metrics	12
Figure S1. Comparison of our approach with traditional methods of identifying climate signals . .	13
Figure S2. Comparison of climwin output across growth metrics for the temperature variable group at Little Tesuque (New Mexico, USA)	14
Figure S3. Comparison of climwin output across growth metrics for the precipitation variable group at Little Tesuque (New Mexico, USA)	15
Figure S4. Comparison of climwin output across growth metrics for the precipitation variable group at Harvard Forest (Massachusetts, USA)	16
Figure S5. Best GLS models for Barro Colorado Island (Panama)	17
Figure S6. Best GLS models for Huai Kha Khaeng (Thailand)	18
Figure S7. Best GLS models for Little Tesuque (New Mexico, USA)	19
Figure S8. Best GLS models for Cedar Breaks (Utah, USA)	20
Figure S9. Best GLS models for SCBI (Virginia, USA)	21
Figure S10. Best GLS models for Lilly Dickey Woods (Indiana, USA)	22
Figure S11. Best GLS models for Harvard Forest (Massachusetts, USA)	23
Figure S12. Best GLS models for Niobrara/ Hansley (Nebraska, USA)	24
Figure S13. Best GLS models for Zofin (Czech Republic)	25
Figure S14. Best GLS models for Scotty Creek (NW Territories, Canada)	26
SI References	27

Appendix S1. Methods for reconstruction of DBH

This is still rough/ mostly notes.

For each core, *DBH* can be reconstructed outside-in (based on recent *DBH*, subtracting growth recorded in tree rings) or inside-out (summing Δr from the inside out). We generally gave precedence to the outside-in approach. Specifically, when *DBH* was taken at the time of coring,

At some of our sites where *DBH* was not taken at the time of coring (*SCBI*), *DBH* measurements taken before or slightly after the time of coring could be used. (see issue #19 in ForestGEO_dendro) If before, ... If after... For all outside-in reconstructions, if a negative *DBH* was predicted...

When there were more than one cores for a tree, the *DBH* reconstructions from each core were averaged to produce a single estimate of the tree's *DBH* through time. When the start or end dates of the records from the cores differed, we extrapolated growth of the shorter core to match the years covered by the longer core. Specifically, to fill in years at the more recent end, we assumed that the average growth rate of the ten years prior to the missing records applied to the missing years. To fill in years at the beginning of the tree's lifespan, we likewise assumed that the ten years adjacent to the missing record applied to the missing years; however, if this yielded a negative *DBH* estimate for the earliest year in the reconstruction, we divided the existing minimum *DBH* by number of years missing and applied that value to each year. We note that these reconstructed growth records were used only for the reconstruction of *DBH* and were not included as response variables in any of our analyses.

In either case we need bark thickness—ideally allometries describing the relationship between *DBH* and bark thickness (Table S4). This is especially critical for thick-barked species. When bark thickness data were available, we generated allometries (issue #8 in ForestGEO_dendro)... lognormal model with intercept forced to zero: `lm(bark_depth.mm ~ -1 + log(dbh_no_bark.cm+1):bark_species, data = bark)`. When bark thickness data were not available, we used published bark allometries from other sources (Table S4)

Appendix S2. Methods for comparing climwin results with traditional methods

(ISSUE #35 in ForestGEO-climate-sensitivity)

To verify that our methods gave similar results to traditional methods, we conducted qualitative comparisons of our results to previous studies based on the same cores (Table S5). We also conducted a formal comparison using identical tree-ring and climate data for four well-studied species: PSME (Cedar Breaks, Utah), ABAL (Zofin), PIMA (Scotty Creek), and LITU (SCBI) (Fig. S1). We compared results from an analysis using conventional methods, as detailed below, to an analysis using our method as described in the Methods section, but with the *climwin* climate variable selection process limited to just the species of interest (as opposed to all species at the site), climate variables considered individually rather than additively, and with start date adjusted to match the conventional method.

The ring-width series from each core was standardized via ARSTAN using a 2/3rds n spline, where n is the number of years in the series (Cook, 1985; Cook & Kairiukstis, 1990- citations in Helcoski). (*The following italic text is plagiarized from Helcoski and needs to be reworded:*) *The influence of outliers in all series was reduced using the adaptive power transformation, which also stabilises the variance over time (Cook & Peters, 1997). Next, each series was stabilised using either the average correlation between raw ring-width series (r_{bar}) method or a 1/3rds spline method to adjust changes in variance as series replication decreased towards the earlier portion of each chronology (Jones et al., 1997). The 1/3rds spline method was chosen when replication in the inner portion of each chronology (c. the inner 30–50 yr of each record depending on full chronology length) dropped below three trees. Once that step was complete, a robust biweight mean chronology for each species was calculated from the ring-width indices (Cook, 1985). We chose to use residual chronologies because the autoregressive standardisation process in creating them removes much of the tree-level autocorrelation in growth and these chronologies would most likely contain the most conservative information on drivers of interannual growth (Cook, 1985).*

Following Helcoski et al. (2019), we defined chronology start dates according to the subsample signal strength (SSS), using a cutoff of $\text{SSS} = 0.80$ (or 80% of the population signal). Thus, for this analysis only, we defined chronology start dates as the year the SSS exceeded 0.80 or two years after the start of the climate record, whichever came later. SSS exceeded 0.80 well before the start of the 1901 start of climate records for PSME (1800s), ABAL (1700), and PIMA (1850s). For LITU, SSS reached 0.8 with 11 trees in 1919, which we used as the start date for this series. We note that these start date criteria differ from those used in the main analysis (Table S3), which had earlier start dates because the analysis was not constrained by a need to represent the full population signal. End dates were defined as the last full year prior to sampling (Table S3).

Appendix S3. Dealing with rapidly changing climate and tree growth

ISSUE #25 in ForestGEO-climate-sensitivity

Our analysis included two sites where climate change has had pronounced effects on tree growth: Scotty Creek, NW Territories, Canada (SC) and Little Tesuque, New Mexico, USA (LT). At SC, [temperatures have increased by X ° over X years]..., resulting in negative growth trends in basal area index (*BAI*) starting around 1950 and significant growth declines since 1970 in 56% of trees (Sniderhan & Baltzer, 2016). At LT, (*drought has increased dramatically*), resulting in many missing rings in recent years.

This is in process. We will try and compare 3 methods: (1) our standard approach, (2) detrending the climate variables (#53), (3) applying the climwin step only for older records--before the most rapid climate change. We will work with SC and LT researchers to determine which makes most sense, and use that as the main approach for these sites.

Table S1. Site Details

site code	site name	latitude	longitude	elevation (m.a.s.l.)	cores within ForestGEO plot?	canopy positions	tree statuses	date range	dormant season	months in climwin
BCI	Barro Colorado Island	9.15430	-79.8461	120-160	no	canopy	live, dead	1931-2014	Nov-Apr	pOct-cDec
HKK	Huai Kha Khaeng	15.63240	99.2170	549-638	no	all	live	1903-2011	Nov-Apr	pOct-cDec
LT	Little Tesuque	35.73838	-105.8382	n.a.	n.a.	all	live	1903-2018		pMay-cAug
CB	Utah Forest Dynamics Plot	37.66150	-112.8525	3020-3169	yes		live	1903-2007		pMay-cAug
SCBI	Smithsonian Conservation Biology Institute	38.89350	-78.1454	273-338	yes	all	live, dead	1903-2017	Oct-Apr	pMay-cAug
LDW	Lilly Dickey Woods	39.23590	-86.2181	230-303		canopy	live, dead	1903-2019		pMay-cAug
HF	Harvard Forest	42.53880	-72.1755	340-368	yes	all	live, dead	1903-2014		pMay-cAug
NE	Niobrara/Halsey	42.78000	-100.0210	644-702	some	canopy	live		Oct-Apr	pMay-cAug
ZOF	Zofin Forest Dynamics Plot	48.66380	14.7073	736-829	some	all	live, dead	1903-2013	Oct-Mar	pMay-cAug
SC	Scotty Creek	61.30000	-121.3000	258-274	no	all	live, dead	1903-2013		pMay-cAug

Table S2. Species analyzed, their characteristics, and bark allometries applied

(ISSUE #72 in ForestGEO-climate-sensitivity)

NOTE: bark.allometry field is not yet right– we will have just one latin name per site, corresponding to allometries in Table S4. But it does give correct info for what is currently applied. We also intend to find and apply more allometries.

species code	family	latin name	sites sampled	leaf type	leaf phenology	light requirements	bark allometry
ABAL	Pinaceae	Abies alba	ZOF	needleleaf	evergreen		neglected in Zofin
ABBI	Pinaceae	Abies bifolia	CB	needleleaf	evergreen		neglected in Cedar Breaks
ACRU	Sapindaceae	Acer rubrum	HF	broadleaf	deciduous (cold)		acru in Harvard
ACSA	Sapindaceae	Acer saccharum	LDW	broadleaf	deciduous (cold)		acru in Lilly Dickey, acru in Lilly Dickey
AFXY	Fabaceae	Afzelia xylocarpa	HKK	broadleaf	deciduous (drought)		neglected in HKK
BEAL	Betulaceae	Betula alleghaniensis	HF	broadleaf	deciduous (cold)		neglected in Harvard
CACO	Juglandaceae	Carya cordiformis	SCBI	broadleaf	deciduous (cold)		caco in SCBI
CAGL	Juglandaceae	Carya glabra	SCBI	broadleaf	deciduous (cold)		cagl in SCBI
CAOV	Juglandaceae	Carya ovata	LDW	broadleaf	deciduous (cold)		cagl in Lilly Dickey
CAOVL	Juglandaceae	Carya ovalis	SCBI	broadleaf	deciduous (cold)		caovl in SCBI
CATO	Juglandaceae	Carya tomentosa	SCBI	broadleaf	deciduous (cold)		cato in SCBI
CHTA	Meliaceae	Chukrasia tabularis	HKK	broadleaf	brevi-deciduous (drought)		neglected in HKK
FAGR	Fagaceae	Fagus grandifolia	HF, SCBI	broadleaf	deciduous (cold)		neglected in Harvard, neglected in Lilly Dickey, neglected in SCBI
FASY	Fagaceae	Fagus sylvatica	ZOF	broadleaf	deciduous (cold)		neglected in Zofin
FRAM	Oleaceae	Fraxinus americana	LDW, SCBI	broadleaf	deciduous (cold)		fram in Lilly Dickey, fram in SCBI
FRNI	Oleaceae	Fraxinus nigra	SCBI	broadleaf	deciduous (cold)		fram in SCBI
JACO	Bignoniaceae	Jacaranda copaia	BCI	broadleaf	deciduous (drought)	light-demanding	JCO in BCI
JUNI	Juglandaceae	Juglans nigra	SCBI	broadleaf	deciduous (cold)		juni in SCBI
LITU	Magnoliaceae	Liriodendron tulipifera	LDW, SCBI	broadleaf	deciduous (cold)		litu in Lilly Dickey, litu in Lilly Dickey, litu in SCBI
MEAZ	Meliaceae	Melia azedarach	HKK	broadleaf	deciduous (drought)	light-demanding	neglected in HKK
PIAB	Pinaceae	Picea abies	HF	needleleaf	evergreen		neglected in Harvard, neglected in Zofin
PIFL	Pinaceae	Pinus flexilis	CB	needleleaf	evergreen		Pinus monticola in Cedar Breaks
PILO	Pinaceae	Pinus longaeva	CB	needleleaf	evergreen		neglected in Cedar Breaks
PIMA	Pinaceae	Picea mariana	SC	needleleaf	evergreen		PIMA in Scotty Creek
PIPO	Pinaceae	Pinus ponderosa	LT	needleleaf	evergreen		Pinus jeffreyi in Little Tesuque, Pinus jeffreyi in NB
PIST	Pinaceae	Pinus strobus	HF, SCBI	needleleaf	evergreen		neglected in Harvard, pist in SCBI
PIST2	Pinaceae	Pinus strobiformis	LT	needleleaf	evergreen		Pinus monticola in Little Tesuque
PSME	Pinaceae	Pseudotsuga menziesii	CB	needleleaf	evergreen		PSME in Cedar Breaks
QUAL	Fagaceae	Quercus alba	LDW, SCBI	broadleaf	deciduous (cold)		qual in Lilly Dickey, qual in SCBI
QUMO	Fagaceae	Quercus montana	LDW, SCBI	broadleaf	deciduous (cold)		qupr in Lilly Dickey, qupr in SCBI
QURU	Fagaceae	Quercus rubra	HF, LDW, SCBI	broadleaf	deciduous (cold)		quru in Harvard, quru in Lilly Dickey, quru in SCBI
QUVE	Fagaceae	Quercus velutina	LDW, SCBI	broadleaf	deciduous (cold)		quve in Lilly Dickey, quve in SCBI
TEPA	Burseraceae	Tetragastris panamensis	BCI	broadleaf	evergreen	shade-tolerant	TPA in BCI
TOCI	Meliaceae	Toona ciliata	HKK	broadleaf	deciduous (drought)		neglected in HKK
TRTU	Meliaceae	Trichilia tuberculata	BCI	broadleaf	evergreen	shade-tolerant	TTU in BCI
TSCA	Pinaceae	Tsuga canadensis	HF	needleleaf	evergreen		neglected in Harvard

*Bark allometry field indicates the species and site sampled to construct the bark allometry. When neither raw data nor an allometric equation for the study species was available, we selected the most appropriate equation that could be located for similar species. Equations are given in Table S4.

Table S3. Sampling details for species by site*(ISSUE #73 in ForestGEO-climate-sensitivity)*

site	species code	n trees all	n cores all	n trees dbh	n cores dbh	dbh range sampled	dbh range reconstructed*	date range
BCI	JACO	12	18	11	17	30.2-63.5	3.8-59.4	1931-2014
BCI	TEPA	18	29	17	26	22.1-59.5	2.6-51.2	1931-2014
BCI	TRTU	23	37	20	31	20.7-43.6	5.3-42.4	1931-2014
CB	PIFL	9	13	NA	NA	NA	NA	1903-2007
CB	PILO	11	12	NA	NA	NA	NA	1903-2007
CB	PSME	10	13	NA	NA	NA	NA	1903-2007
HF	ACRU	18	59	18	59	10.1-22.1	1-20.4	1903-2013
HF	BEAL	13	44	13	44	10.2-37.9	1.6-20.5	1904-2013
HF	QURU	74	180	73	177	19.5-53	1.6-48.3	1903-2014
HF	TSCA	32	83	32	83	10.6-37	0.6-34.4	1923-2014
HKK	AFXY	39	127	39	127	20.1-98.7	0.1-81.4	1903-2011
HKK	CHTA	28	70	28	70	16-64.6	0.2-59.5	1904-2010
HKK	MEAZ	46	130	46	130	25.6-98.1	3.8-80.3	1914-2011
HKK	TOCI	45	143	45	143	16.6-116.4	1.7-80.5	1903-2011
LDW	ACSA	35	66	34	64	9-64.6	0-53.4	1903-2019
LDW	CAOV	9	18	8	16	NA-NA	0.6-38.3	1903-2013
LDW	LITU	15	28	14	26	NA-NA	1.4-70.5	1903-2019
LDW	QUAL	10	20	NA	NA	NA	NA	1903-2013
LDW	QUMO	10	20	8	16	NA-NA	1.4-54.1	1903-2013
LDW	QUVE	9	18	NA	NA	NA	NA	1903-2013
LT	PIPO	10	20	10	20	23.2-52.8	13.3-48.5	1903-2018
LT	PIST2	7	14	7	10	25.7-39.8	3.5-34.4	1903-2018
SCBI	CACO	15	15	15	15	10.62-38.52	2.6-32.3	1903-2015
SCBI	CAGL	39	39	36	36	10.28-52.31	1.6-50.5	1903-2015
SCBI	CAOVL	25	25	24	24	15.11-60.32	2.7-48.4	1903-2015
SCBI	CATO	15	15	14	14	12.86-35.95	4.6-29.5	1903-2015
SCBI	FAGR	76	76	76	76	10.05-41.02	0.1-41.2	1920-2009
SCBI	FRAM	66	66	63	63	6.85-94.73	0.2-86.4	1903-2016
SCBI	FRNI	12	12	12	12	11.04-39.2	1.5-28.4	1903-1996
SCBI	JUNI	30	30	29	29	20.4-76.19	5.9-61.2	1903-2010
SCBI	LITU	106	106	105	105	10-91.42	0.1-82.2	1903-2010
SCBI	PIST	36	36	36	36	13.92-50.96	1.6-45.2	1931-2010
SCBI	QUAL	66	66	66	66	11.4-76.73	0.4-72.3	1903-2009
SCBI	QUMO	67	67	67	67	10.22-84.59	0.4-71.2	1903-2017
SCBI	QURU	71	71	70	70	11.07-87.65	2.6-79.5	1903-2016
SCBI	QUVE	82	82	81	81	16.02-82.33	0.6-79.4	1903-2009
SC	PIMA	443	443	395	395	7-24	0.1-18.5	1903-2013
ZOF	ABAL	55	55	52	52	41-121	21.3-108.5	1903-2011
ZOF	FASY	1369	1369	1368	1368	NA-NA	0.1-115.3	1903-2013
ZOF	PCAB	644	644	635	635	NA-NA	0-126.4	1903-2011

*Maximum reconstructed DBH's analyzed are less than maximum sampled DBH's because we discard size ranges with < 3 conspecific trees.

Table S4. Allometric equations for bark thickness

species	equation	n	DBH.range.cm	site	source
<i>Acer rubrum</i>	$bark.mm = 0.619 * \log(dbh.cm + 1)$	10	8.2-39.6	SCBI	Anderson-Teixeira et al. (2015)
<i>Carya cordiformis</i>	$bark.mm = 0.793 * \log(dbh.cm + 1)$	9	5.9-68.2	SCBI	Anderson-Teixeira et al. (2015)
<i>Carya ovalis</i>	$bark.mm = 1.531 * \log(dbh.cm + 1)$	8	6.4-63.1	SCBI	Anderson-Teixeira et al. (2015)
<i>Carya ovata</i>	$bark.mm = 1.035 * \log(dbh.cm + 1)$	8	19.1-78	SCBI	Anderson-Teixeira et al. (2015)
<i>Carya tomentosa</i>	$bark.mm = 1.105 * \log(dbh.cm + 1)$	8	5-57.3	SCBI	Anderson-Teixeira et al. (2015)
<i>Fraxinus americana</i>	$bark.mm = 2.223 * \log(dbh.cm + 1)$	9	6.1-94.2	SCBI	Anderson-Teixeira et al. (2015)
<i>Jacaranda copaia</i>	$bark.mm = 2.993 * \log(dbh.cm + 1)$	5	45.6-75	Panama	Raquel Alfaro-Sanchez (unpublished data)
<i>Juglans nigra</i>	$bark.mm = 2.107 * \log(dbh.cm + 1)$	9	13.6-85.4	SCBI	Anderson-Teixeira et al. (2015)
<i>Liriodendron tulipifera</i>	$bark.mm = 1.637 * \log(dbh.cm + 1)$	9	27.5-136.5	SCBI	Anderson-Teixeira et al. (2015)
<i>Picea mariana</i>	$bark.mm = 3.726 * \log(dbh.cm + 1)$	12	6.9-7.9	Scotty Creek	Anastasia Sniderhan and Jennifer Baltzer (unpublished data)
<i>Pinus flexilis</i>	$bark.mm = (1.299 * \sqrt{dbh.cm})^{0.609})^2$	29	10-130	California (3 montane sites)	Zeibig-Kichas et al. (2016)
<i>Pinus ponderosa</i>	$bark.mm = (1.298 * \sqrt{dbh.cm})^{0.802})^2$	81	5-160	California (4 montane sites)	Zeibig-Kichas et al. (2016)
<i>Pinus strobus</i>	$bark.mm = 1.568 * \log(dbh.cm + 1)$	1	28.4-28.4	Illinois	Miles and Smith (2009)
<i>Pseudotsuga menziesii</i>	$bark.mm = (0.785 * \sqrt{dbh.cm})^2$	30	10-200	California (3 montane sites)	Zeibig-Kichas et al. (2016)
<i>Quercus alba</i>	$bark.mm = 1.828 * \log(dbh.cm + 1)$	10	9.3-101.8	SCBI	Anderson-Teixeira et al. (2015)
<i>Quercus montana</i>	$bark.mm = 2.083 * \log(dbh.cm + 1)$	8	5.8-99.1	SCBI	Anderson-Teixeira et al. (2015)
<i>Quercus rubra</i>	$bark.mm = 0.98 * \log(dbh.cm + 1)$	10	24.1-143.2	SCBI	Anderson-Teixeira et al. (2015)
<i>Quercus velutina</i>	$bark.mm = 1.394 * \log(dbh.cm + 1)$	8	16.2-110.7	SCBI	Anderson-Teixeira et al. (2015)
<i>Tetragastris panamensis</i>	$bark.mm = 1.672 * \log(dbh.cm + 1)$	4	22.7-48.8	Panama	Raquel Alfaro-Sanchez (unpublished data)
<i>Trichilia tuberculata</i>	$bark.mm = 1.367 * \log(dbh.cm + 1)$	12	21-40.5	Panama	Raquel Alfaro-Sanchez (unpublished data), Pete Kerby-Miller and Helene Muller-Landau (unpublished data)

For assignments of species as proxies for those with out available bark allometries, see Table S2.

Table S5. Qualitative comparison of results from this study with previous studies employing conventional methods

species	Precipitation response		Temperature response		reference
	previously observed	observed here	previously observed	observed here	
Barro Colorado Island, Panama					
JACO	pos. correlation to Apr-Dec <i>PPT</i> (strongest of the 3 species)	pos. correlation to Mar-Dec <i>PPT</i> (strongest of the 3 species)	no sig. correlation to annual T_{mean} or T_{min}	neg. response to Feb-Mar T_{min}	Alfaro-Sánchez et al. 2017
TEPA	pos. correlation to Apr-Dec <i>PPT</i> (response weaker than JACO, similar to TRTU)	pos. correlation to Mar-Dec <i>PPT</i> (response weaker than JACO, similar to TRTU)	no sig. correlation to annual T_{mean} or T_{min}	no sig. correlation to Feb-Mar T_{min}	Alfaro-Sánchez et al. 2017
TRTU	pos. correlation to Apr-Dec <i>PPT</i> (response weaker than JACO, similar to TEPA)	pos. correlation to Mar-Dec <i>PPT</i> (response weaker than JACO, similar to TEPA)	no sig. correlation to annual T_{mean} or T_{min}	non-sig. slight pos. response to Feb-Mar T_{min}	Alfaro-Sánchez et al. 2017
Huai Kha Khaeng, Thailand					
AFXY	sig. pos. correlation with June <i>PPT</i> , otherwise n.s.	slight concave-down response to p.Sept-June <i>PPT</i> frequency	sig. neg. correlation with T_{max} in Aug and Dec; T_{min} in p.Oct., Jul, Aug	slight concave-down response to Apr-Oct T_{max}	Vlam et al. 2013
CHTA	sig. pos. correlation with April <i>PPT</i> , otherwise n.s.	slight concave-down response to p.Sept-June <i>PPT</i> frequency	sig. neg. correlation with T_{max} in May, Aug-Sept; T_{min} in Feb, May, Aug	slight neg. response to Apr-Oct T_{max}	Vlam et al. 2013
MEAZ	sig. pos. correlation with April <i>PPT</i> , otherwise n.s.	concave-down response to p.Sept-June <i>PPT</i> frequency	sig. neg. correlation with T_{max} in May-Aug; T_{min} in May-Aug	neg. response to Apr-Oct T_{max}	Vlam et al. 2013
TOCI	sig. pos. correlation with p.Oct-p.Nov and April-May <i>PPT</i>	concave-down /increasing response to p.Sept-June <i>PPT</i> frequency	sig. neg. correlation with T_{max} every month from pOct-June (excluding March); T_{min} in Jan and Mar-Aug	neg. response to Apr-Oct T_{max}	Vlam et al. 2013
PIPO				-	
PIST2				-	
				-	

Table S5, cont.

species	Precipitation response		Temperature response		reference
	previously observed	observed here	previously observed	observed here	
Smithsonian Conservation Biology Institute, Virginia, USA					
CACO	pos. correlations with May-Aug <i>PPT</i> (sig. May, July)	NA	neg. correlations with May-Aug <i>PET</i> (sig. May-July)	**(sig or ns)** neg. response to May-July <i>PET</i>	Helcoski et al. 2019
CAGL	pos. correlations with May-Aug <i>PPT</i> (sig. May)	NA	neg. correlations with May-Aug <i>PET</i> (n.s.)	**(sig or ns)** neg. response to May-July <i>PET</i>	Helcoski et al. 2019
CAOVL	pos. correlations with May-Aug <i>PPT</i> (sig. Aug)	NA	neg. correlations with May-Aug <i>PET</i> (sig. all months)	**(sig or ns)** neg. response to May-July <i>PET</i>	Helcoski et al. 2019
CATO	pos. correlations with May-Aug <i>PPT</i> (n.s.)	NA	neg. correlations with May-Aug <i>PET</i> (sig. June)	**(sig or ns)** neg. response to May-July <i>PET</i>	Helcoski et al. 2019
FAGR	pos. correlations with May-Aug <i>PPT</i> (sig. July-Aug)	NA	neg. correlations with May-Aug <i>PET</i> (sig. July-Aug)	**(sig or ns)** neg. response to May-July <i>PET</i>	Helcoski et al. 2019
FRAM	pos. correlations with May-Aug <i>PPT</i> (sig. May-June)	NA	neg. correlations with May-Aug <i>PET</i> (sig. May-June)	**(sig or ns)** neg. response to May-July <i>PET</i>	Helcoski et al. 2019
FRNI	no sig. correlations with peak growing season <i>PPT</i>	NA	no sig. correlations with peak growing season <i>PET</i>	**(sig or ns)** neg. response to May-July <i>PET</i>	Helcoski et al. 2019
JUNI	pos. correlations with May-Aug <i>PPT</i> (sig. Jun-Aug)	NA	neg. correlations with May-Aug <i>PET</i> (sig. July-Aug)	non-sig. neg. response to May-July <i>PET</i>	Helcoski et al. 2019
LITU	pos. correlations with May-Aug <i>PPT</i> (sig. May-July)	NA	neg. correlations with May-Aug <i>PET</i> (sig. all months)	**(sig or ns)** neg. response to May-July <i>PET</i>	Helcoski et al. 2019
PIST	pos. correlations with May-Aug <i>PPT</i> (n.s.)	NA	neg. correlations with May-Aug <i>PET</i> (n.s.)	**(sig or ns)** neg. response to May-July <i>PET</i>	Helcoski et al. 2019
QUAL	pos. correlations with May-Aug <i>PPT</i> (sig. May)	NA	neg. correlations with May-Aug <i>PET</i> (sig. all months)	**(sig or ns)** neg. response to May-July <i>PET</i>	Helcoski et al. 2019
QUMO	pos. correlations with May-Aug <i>PPT</i> (sig. May)	NA	neg. correlations with May-Aug <i>PET</i> (sig. May-June, Aug)	**(sig or ns)** neg. response to May-July <i>PET</i>	Helcoski et al. 2019
QURU	pos. correlations with May-Aug <i>PPT</i> (n.s.)	NA	neg. correlations with May-Aug <i>PET</i> (sig. May, July-Aug)	**(sig or ns)** neg. response to May-July <i>PET</i>	Helcoski et al. 2019
QUVE	pos. correlations with May-Aug <i>PPT</i> (sig. May-July)	NA	neg. correlations with May-Aug <i>PET</i> (sig. all months)	**(sig or ns)** neg. response to May-July <i>PET</i>	Helcoski et al. 2019

Table S5, cont.

species	Precipitation response		Temperature response		reference
	previously observed	observed here	previously observed	observed here	
Lilly Dickey Woods, Indiana, USA					
LITU	pos. correlations with Jun-Aug PDSI	pos. response to June <i>PPT</i>	neg. response to Jun-Aug <i>T_{max}</i>	neg. response to June <i>PET</i>	Maxwell, Harley, and Robeson 2016
QUAL	pos. correlations with Jun-Aug PDSI	pos. response to June <i>PPT</i>	neg. response to Jun-Aug <i>T_{max}</i>	neg. response to June <i>PET</i>	Maxwell, Harley, and Robeson 2016
QUMO	pos. correlations with Jun-Aug PDSI	pos. response to June <i>PPT</i>	neg. response to Jun-Aug <i>T_{max}</i>	neg. response to June <i>PET</i>	Maxwell, Harley, and Robeson 2016
QUVE	pos. correlations with Jun-Aug PDSI	pos. response to June <i>PPT</i>	neg. response to Jun-Aug <i>T_{max}</i>	neg. response to June <i>PET</i>	Maxwell, Harley, and Robeson 2016
					-
					Aus de Ar et al. 2018; Bumann et al. 2019
Žofín Forest Dynamics Plot, Czech Republic					
ABAL	no sig. correlations with June-July <i>PPT</i>	slight concave-down response to p.Jun-p.July <i>PPT</i> frequency	sig. pos. correlation to April T (strongest T correlation)	pos. response to Jan-March <i>T_{max}</i>	Kašpar, Tumajer, Vašíčková, and Šamonil, in review
FASY	no sig. correlations with June-July <i>PPT</i>	pos. response to p.Jun-p.July <i>PPT</i> frequency	sig. pos. correlation to Jan T (strongest T correlation)	pos. response to Jan-March <i>T_{max}</i>	Kašpar, Tumajer, Vašíčková, and Šamonil, in review
PIAB	modest pos. correlations (n.s) with June-July <i>PPT</i>	pos. response to p.Jun-p.July <i>PPT</i> frequency	sig. pos. correlation to March T (strongest current-year T correlation)	pos. response to Jan-March <i>T_{max}</i>	Kašpar, Tumajer, Vašíčková, and Šamonil, in review
	>700m elev. sites moisture limited June-Aug		>700m elev. sites temperature limited except June-Aug		Tumajer et al. 2017
Scotty Creek, NW Territories, Canada					
					Sniderhan and Baltzer 2016

Results from this study are the climate-only model. Where previous studies examined numerous climate variables or time windows (e.g., Helcoski et al., 2019), we focus on those most relevant to our findings. Beyond the methodological differences, original studies vary from this one and from one another in factors including exact set of cores analyzed, climate data sources, time frame of analysis, approaches to identifying candidate climate variables and windows (including whether this is done on a site or species level), methods for detrending and standardizing to build chronologies, and whether the effects of temperature and precipitation are considered separately (original studies) or additively (this study). An analysis standardizing all of these factors for four species is present in Appendix S2 and Fig. S1.

Table S6. Frequency of *DBH*-climate interactions across all sites and growth metrics

Figure S1. Comparison of our approach with traditional methods of identifying climate signals

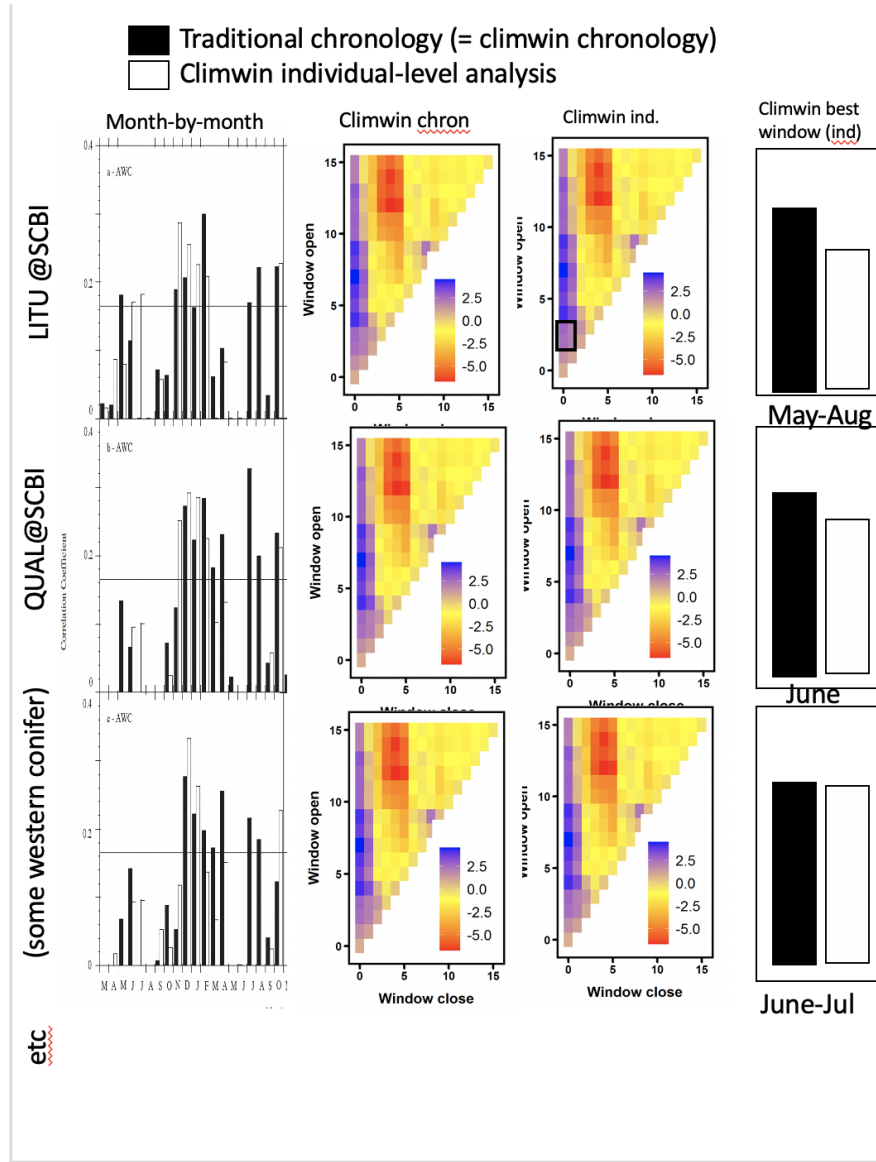


Figure S1 | (Comparison of traditional approaches with ours). (THIS FIGURE IS JUST A MOCK-UP –NOT REAL DATA. REAL FIGURE WILL INCLUDE 3-4 COMMONLY STUDIED SPECIES FROM DIFFERENT SITES.)

Figure S2. Comparison of climwin output across growth metrics for the temperature variable group at Little Tesuque (New Mexico, USA)

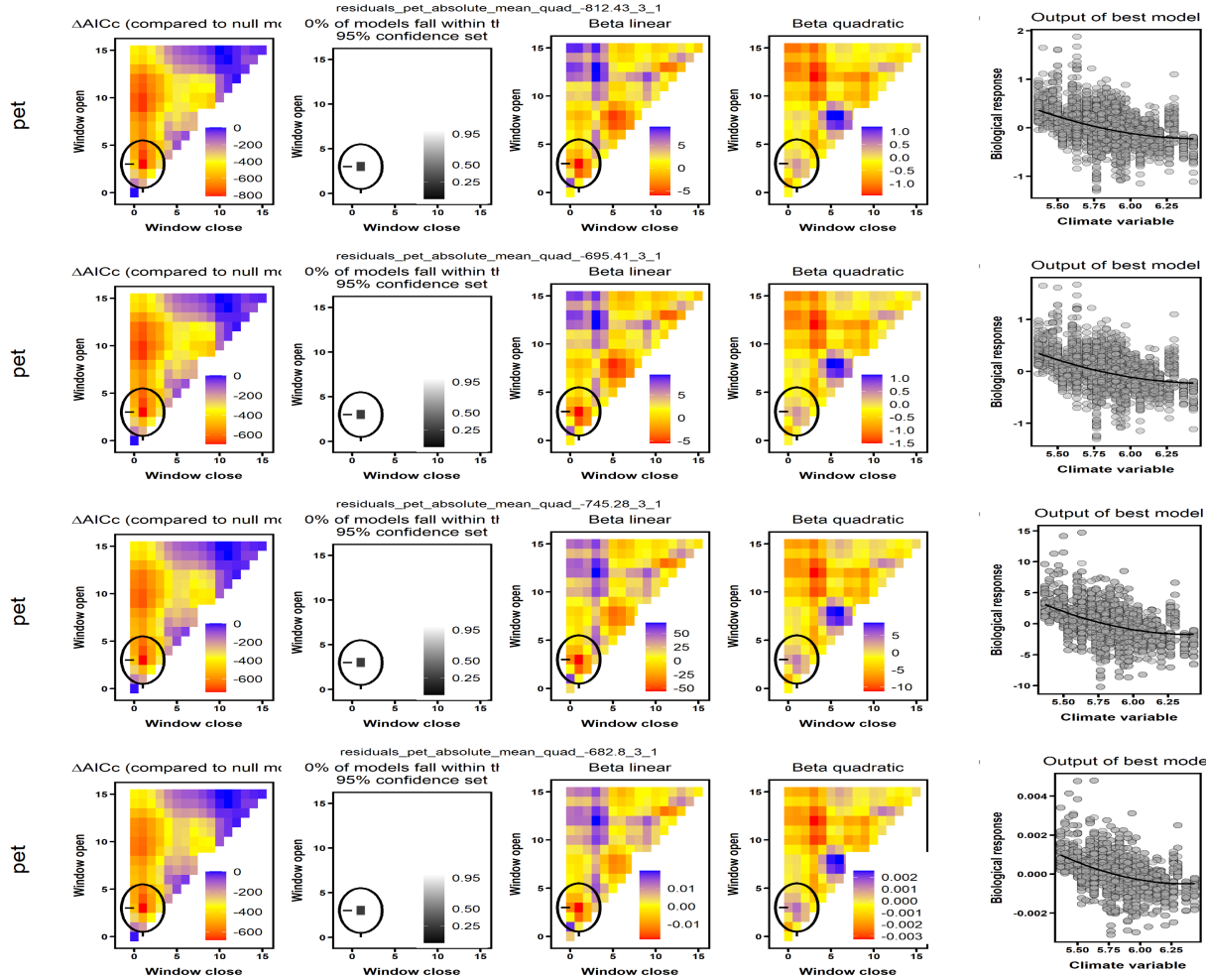


Figure S2 | Comparison of climwin output across growth metrics for the temperature variable group at Little Tesuque (New Mexico, USA). Here, *climwin* identified potential evapotranspiration (*PET*) as the strongest climate variable across all three metrics of growth (Δr , BAI, ΔAGB) and regardless of whether all cores were included in the analysis, or only those for which DBH could be reconstructed (Δr -trees with *DBH*, BAI, ΔAGB).

Figure S3. Comparison of climwin output across growth metrics for the precipitation variable group at Little Tesuque (New Mexico, USA)

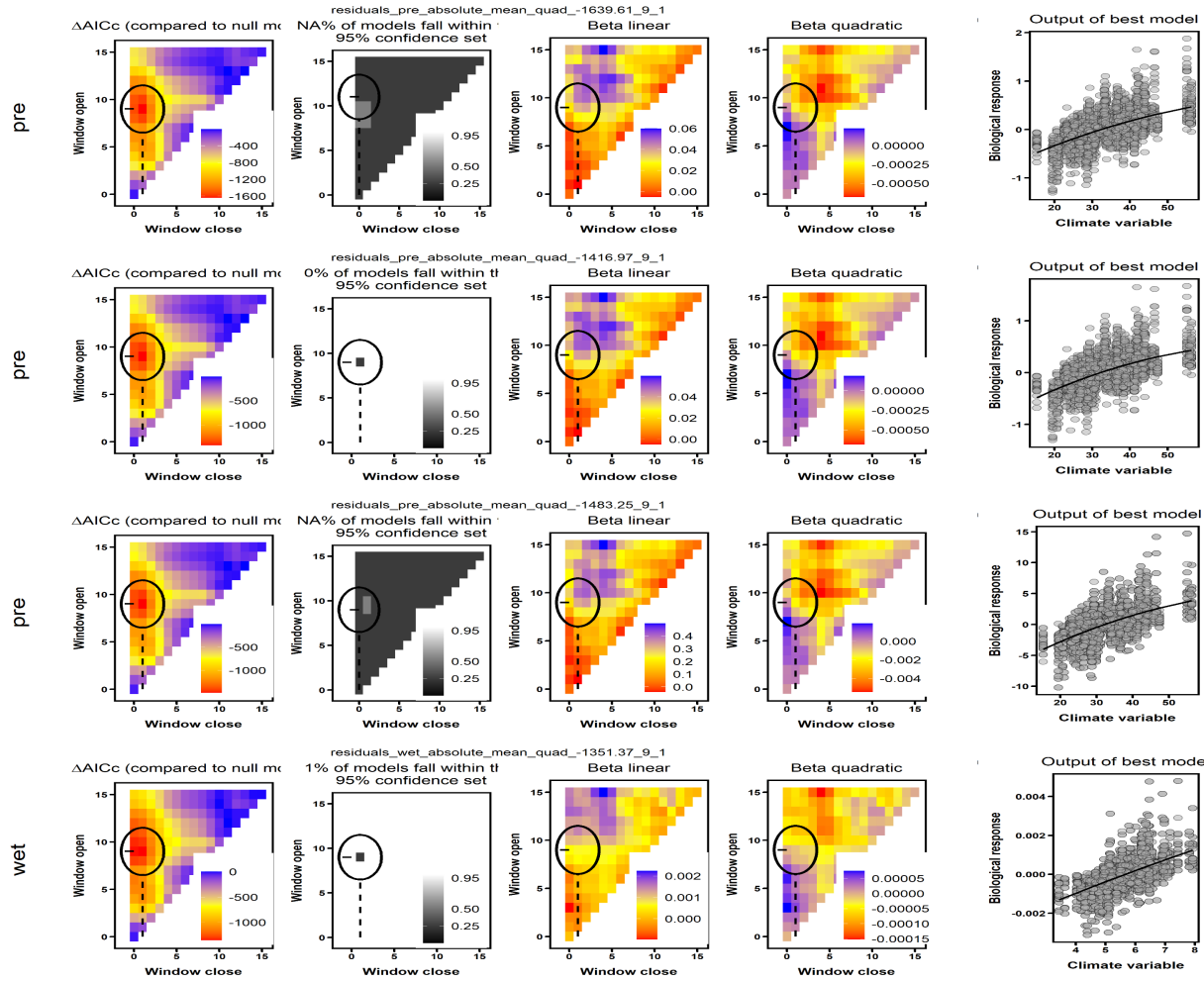


Figure S3 | Comparison of climwin output across growth metrics for the precipitation variable group at Little Tesuque (New Mexico, USA). Here, *climwin* identified precipitation (*PPT*) as the strongest climate variable for Δr and *BAI*, but precipitation day frequency (*PDF*) as the strongest climate variable for ΔAGB .

Figure S4. Comparison of climwin output across growth metrics for the precipitation variable group at Harvard Forest (Massachusetts, USA)

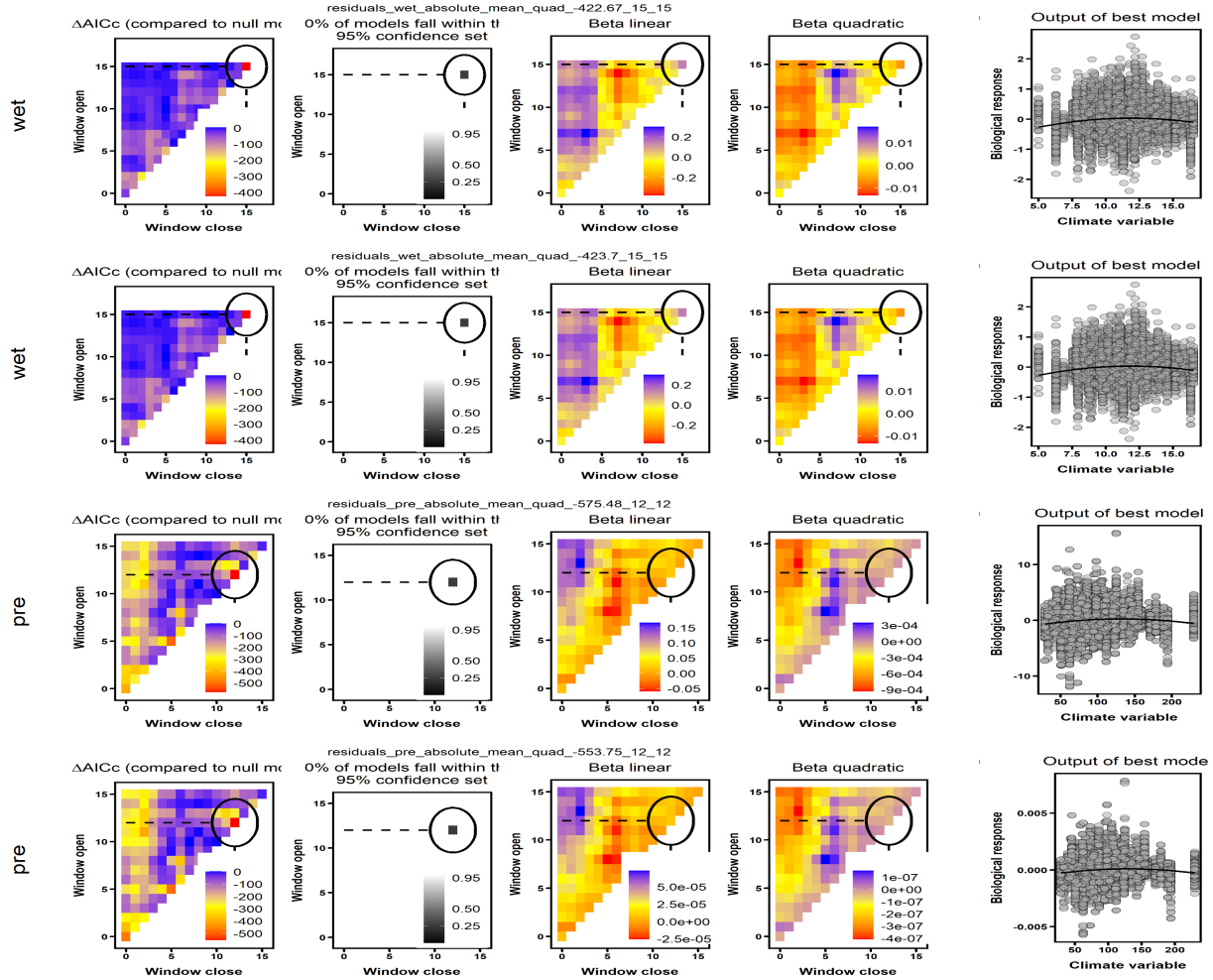


Figure S4 | Comparison of climwin output across growth metrics for the precipitation variable group at Harvard Forest (Massachusetts, USA). Here, *climwin* identified precipitation frequency (*PDF*) as the strongest climate variable for Δr , but precipitation amount (*PPT*) as the strongest climate variable for *BAI* and ΔAGB . The optimal time window (circled) also differed across growth metrics.

Figure S5. Best GLS models for Barro Colorado Island (Panama)

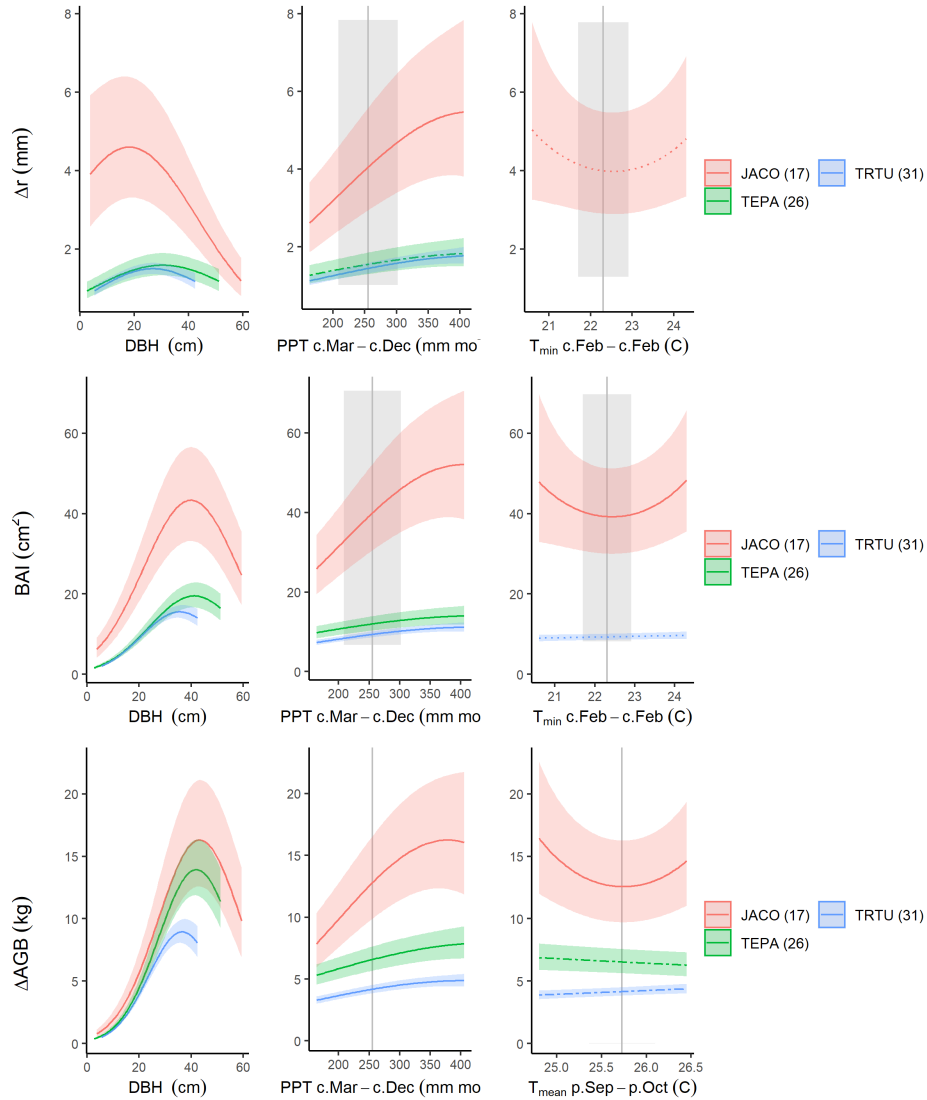


Figure S5 | Best GLS models for Barro Colorado Island (Panama) for all three growth metrics: Δr , BAI, and ΔAGB . Precipitation and temperature group variables are as selected by *climwin* (p=previous year, c=current year). For each species, relationships are plotted if included in top model, with best-fit polynomials plotted with solid lines when both first- and second-order terms are significant, dashed lines when only one term is significant, and dotted lines when neither is significant. Transparent ribbons indicate 95% confidence intervals. Vertical grey lines indicate the long-term mean for the climate variable, shading indicates 1 SD.

Figure S6. Best GLS models for Huai Kha Khaeng (Thailand)

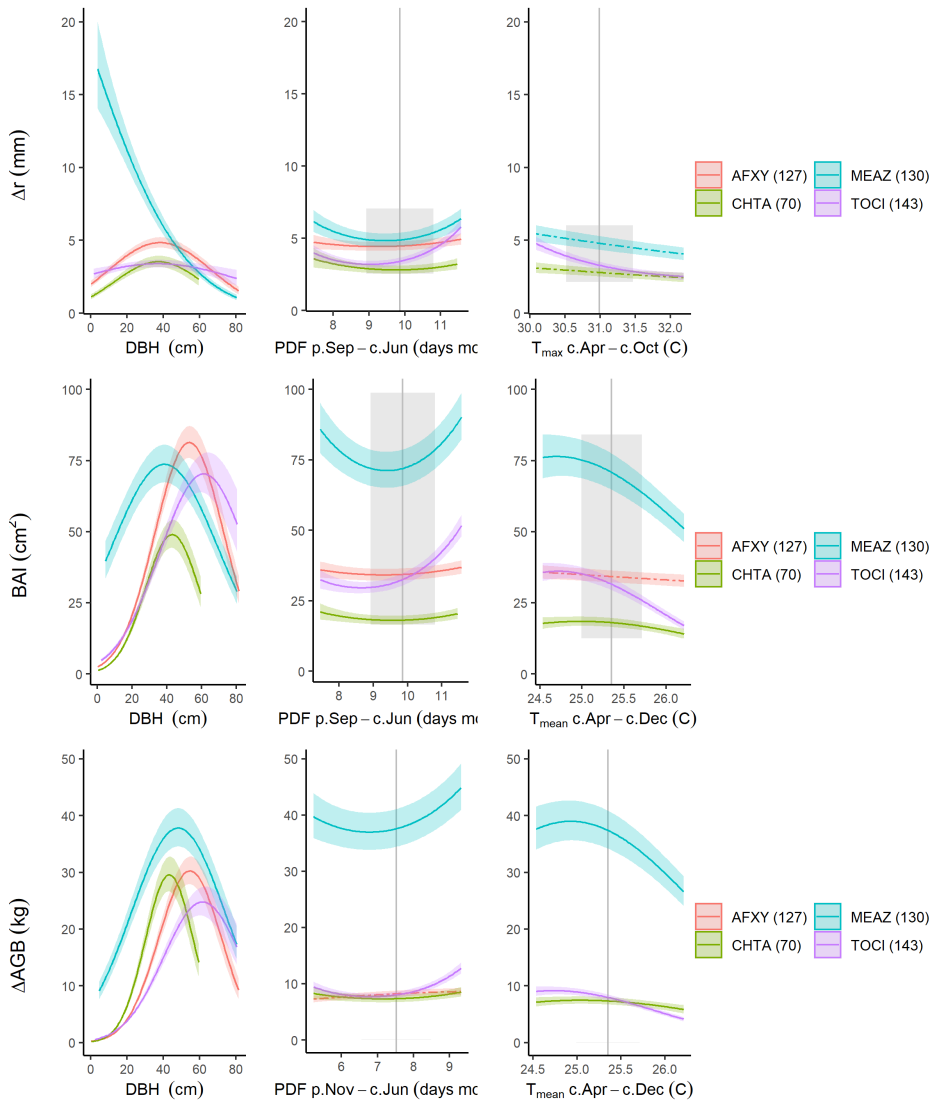


Figure S6 | Best GLS models for Huai Kha Khaeng (Thailand) for all three growth metrics: Δr , BAI , and ΔAGB . Precipitation and temperature group variables are as selected by *climwin* (*p*=previous year, *c*=current year). For each species, relationships are plotted if included in top model, with best-fit polynomials plotted with solid lines when both first- and second-order terms are significant, dashed lines when only one term is significant, and dotted lines when neither is significant. Transparent ribbons indicate 95% confidence intervals. Vertical grey lines indicate the long-term mean for the climate variable, shading indicates 1 SD.

Figure S7. Best GLS models for Little Tesuque (New Mexico, USA)

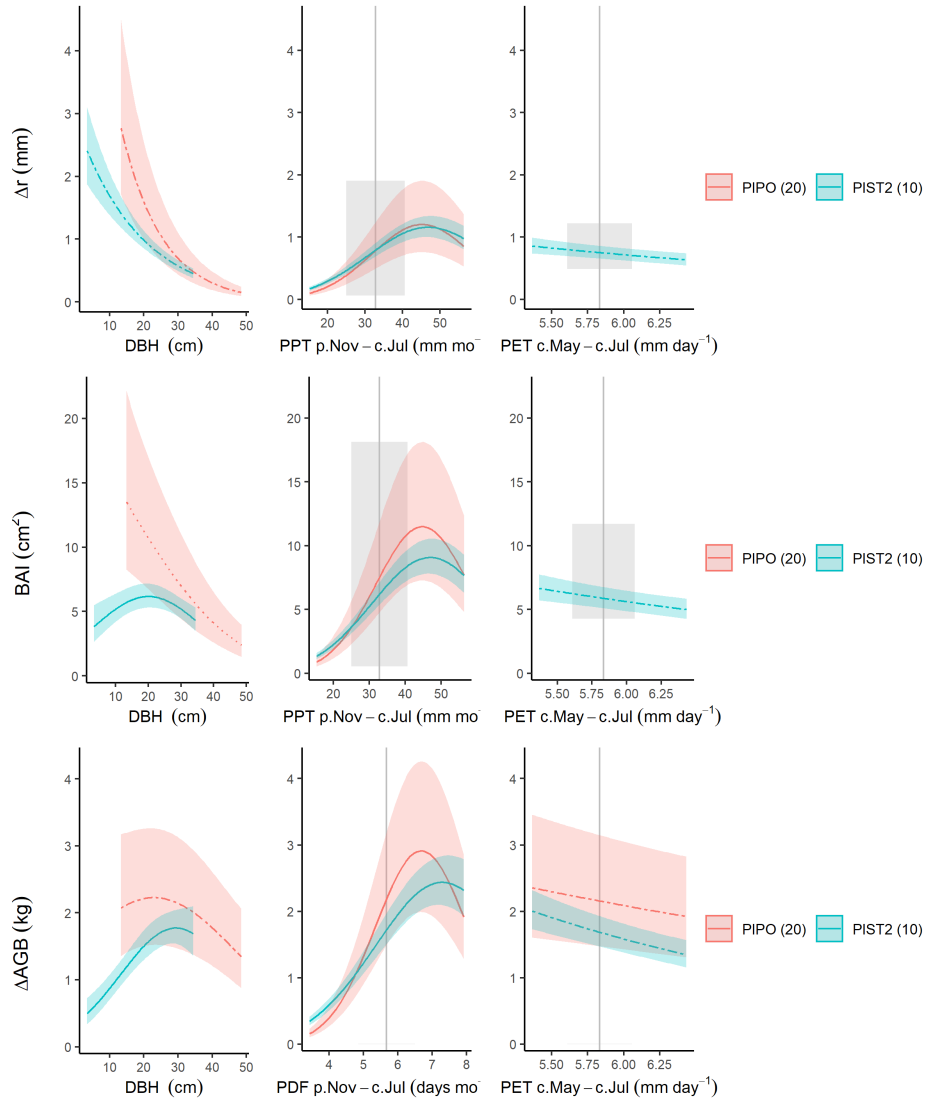


Figure S7 | Best GLS models for Little Tesuque (New Mexico, USA) for all three growth metrics: Δr , BAI , and ΔAGB . Precipitation and temperature group variables are as selected by *climwin* (p =previous year, c =current year). For each species, relationships are plotted if included in top model, with best-fit polynomials plotted with solid lines when both first- and second-order terms are significant, dashed lines when only one term is significant, and dotted lines when neither is significant. Transparent ribbons indicate 95% confidence intervals. Vertical grey lines indicate the long-term mean for the climate variable, shading indicates 1 SD.

Figure S8. Best GLS models for Cedar Breaks (Utah, USA)

[Figure S8 | Best GLS models for Cedar Breaks (Utah, USA) for all three growth metrics: Δr , BAI , and ΔAGB . Precipitation and temperature group variables are as selected by *climwin* (p=previous year, c=current year). For each species, relationships are plotted if included in top model, with best-fit polynomials plotted with solid lines when both first- and second-order terms are significant, dashed lines when only one term is significant, and dotted lines when neither is significant. Transparent ribbons indicate 95% confidence intervals. Vertical grey lines indicate the long-term mean for the climate variable, shading indicates 1 SD.]

Figure S9. Best GLS models for SCBI (Virginia, USA)

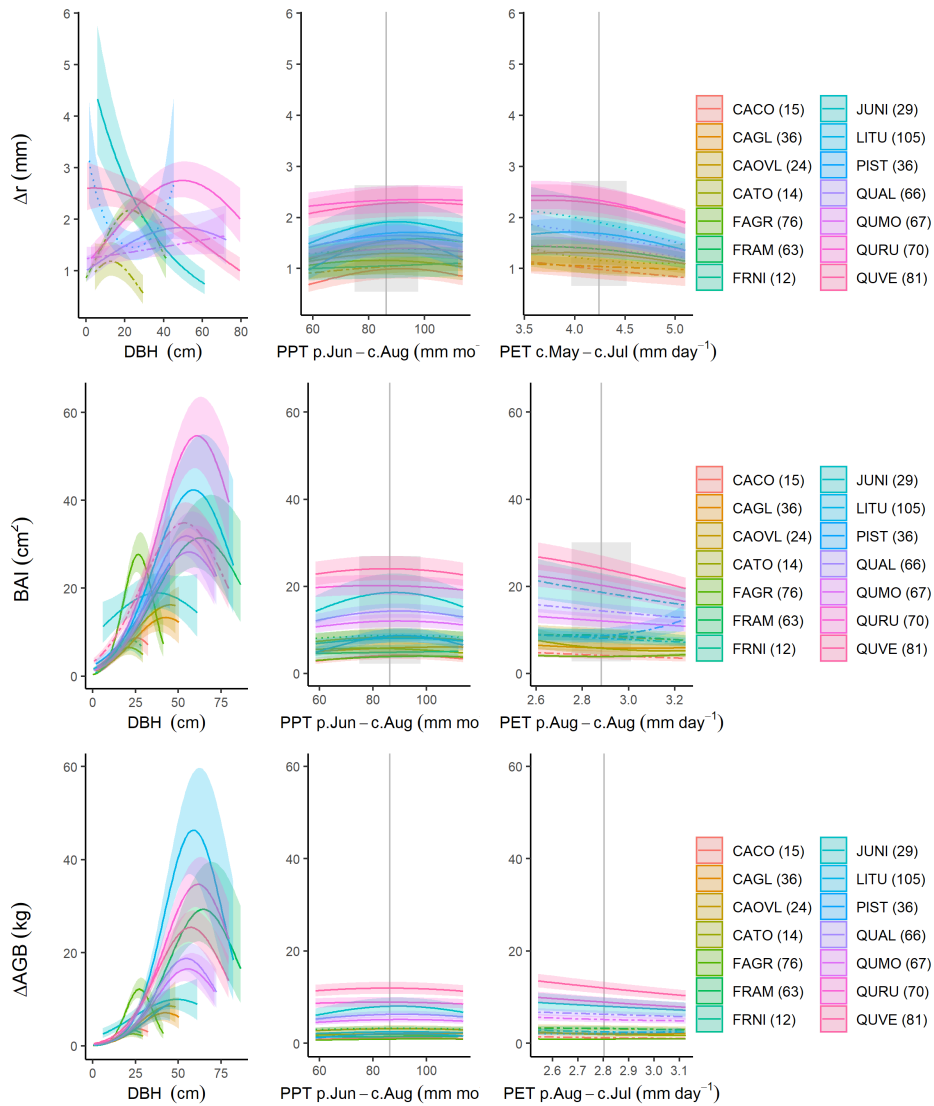


Figure S9 | Best GLS models for SCBI (Virginia, USA) for all three growth metrics: Δr , BAI, and ΔAGB . Precipitation and temperature group variables are as selected by *climwin* (p=previous year, c=current year). For each species, relationships are plotted if included in top model, with best-fit polynomials plotted with solid lines when both first- and second-order terms are significant, dashed lines when only one term is significant, and dotted lines when neither is significant. Transparent ribbons indicate 95% confidence intervals. Vertical grey lines indicate the long-term mean for the climate variable, shading indicates 1 SD.

Figure S10. Best GLS models for Lilly Dickey Woods (Indiana, USA)

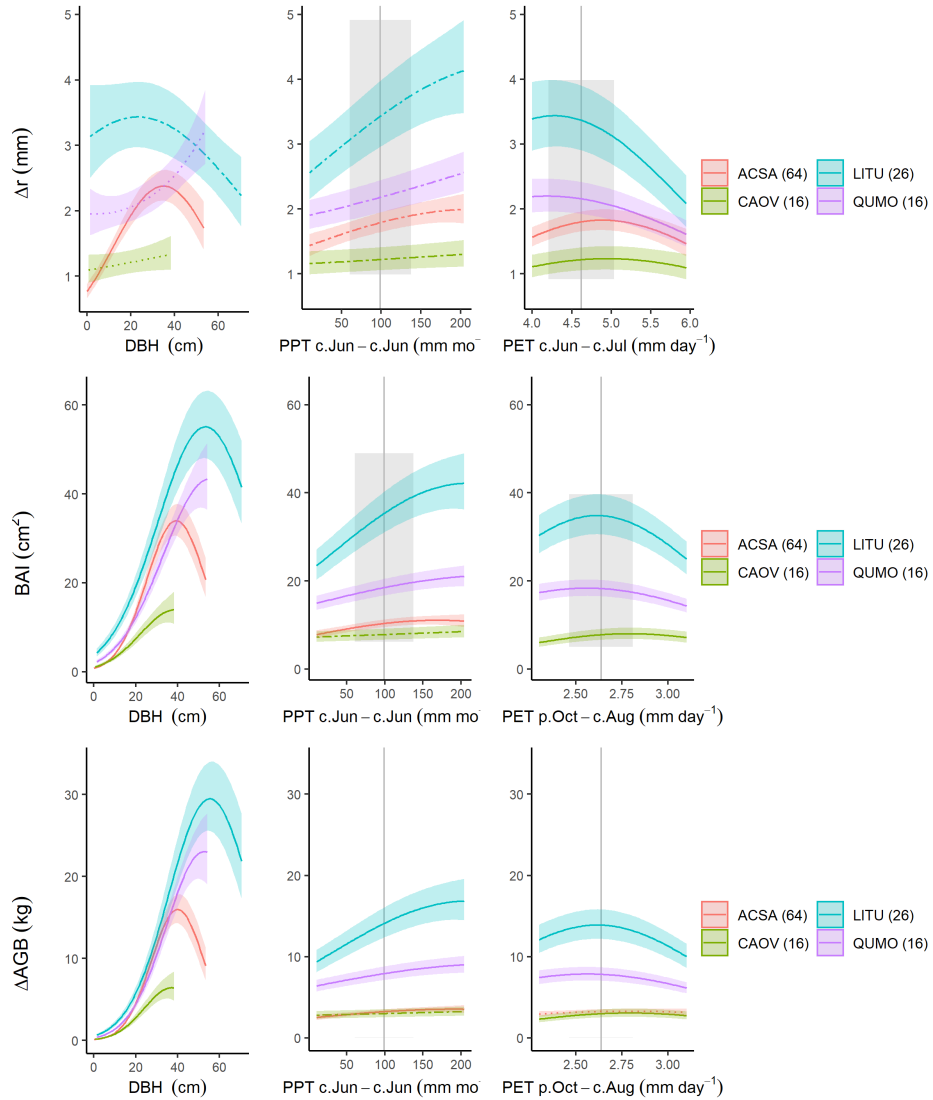


Figure S10 | Best GLS models for Lilly Dickey Woods (Indiana, USA) for all three growth metrics: Δr , BAI , and ΔAGB . Precipitation and temperature group variables are as selected by *climwin* (p =previous year, c =current year). For each species, relationships are plotted if included in top model, with best-fit polynomials plotted with solid lines when both first- and second-order terms are significant, dashed lines when only one term is significant, and dotted lines when neither is significant. Transparent ribbons indicate 95% confidence intervals. Vertical grey lines indicate the long-term mean for the climate variable, shading indicates 1 SD.

Figure S11. Best GLS models for Harvard Forest (Massachusetts, USA)

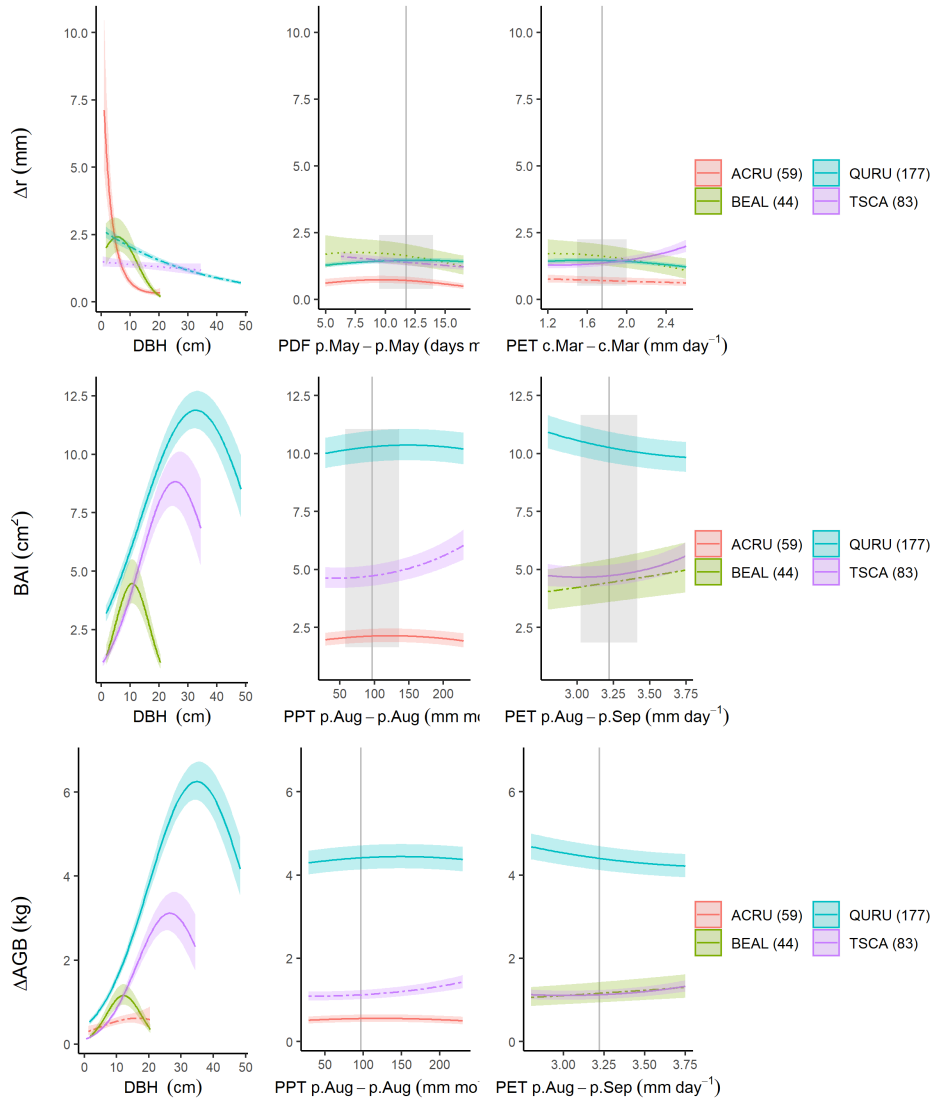


Figure S11 | Best GLS models for Harvard Forest (Massachusetts, USA) for all three growth metrics: Δr , BAI, and ΔAGB . Precipitation and temperature group variables are as selected by *climwin* (*p*=previous year, *c*=current year). For each species, relationships are plotted if included in top model, with best-fit polynomials plotted with solid lines when both first- and second-order terms are significant, dashed lines when only one term is significant, and dotted lines when neither is significant. Transparent ribbons indicate 95% confidence intervals. Vertical grey lines indicate the long-term mean for the climate variable, shading indicates 1 SD.

Figure S12. Best GLS models for Niobrara/ Hansley (Nebraska, USA)

Figure S13. Best GLS models for Zofin (Czech Republic)

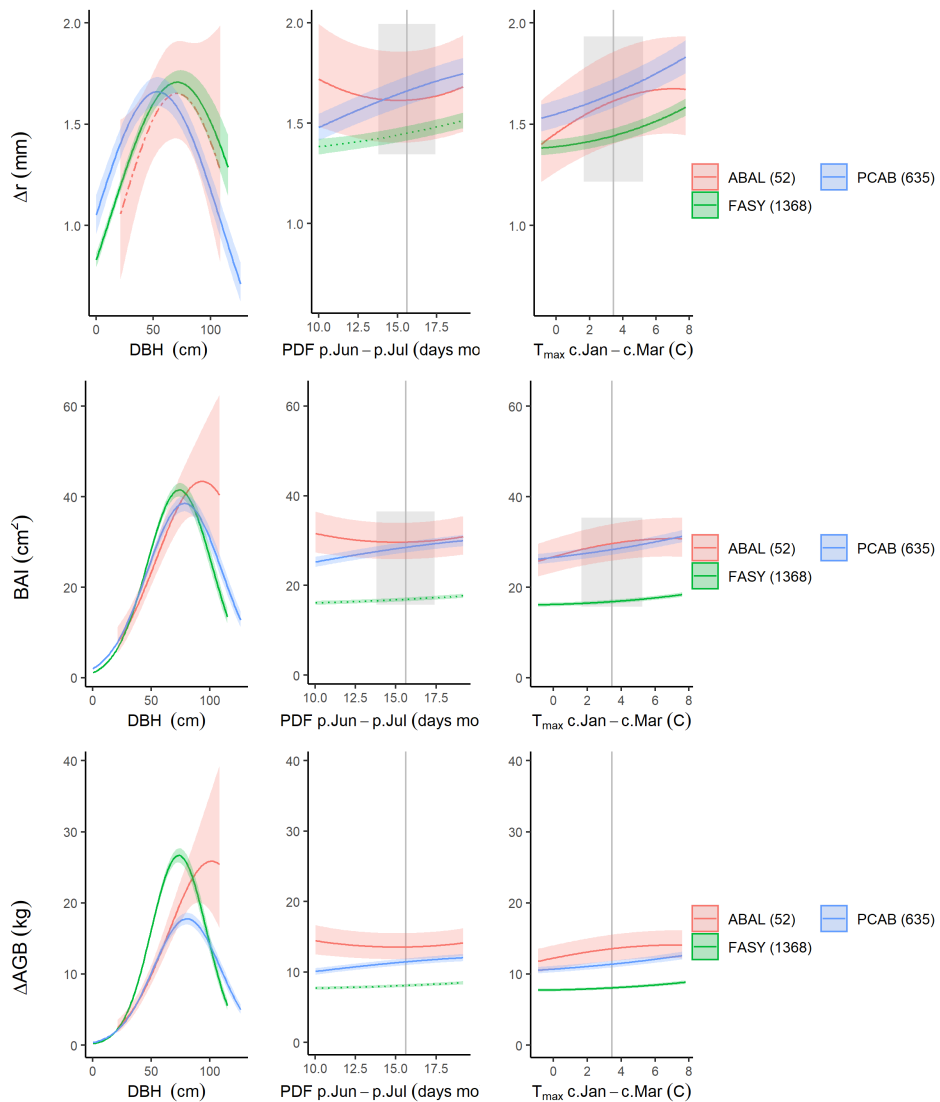


Figure S13 | Best GLS models for Zofin (Czech Republic) for all three growth metrics: Δr , BAI, and ΔAGB . Precipitation and temperature group variables are as selected by *climwin* (p=previous year, c=current year). For each species, relationships are plotted if included in top model, with best-fit polynomials plotted with solid lines when both first- and second-order terms are significant, dashed lines when only one term is significant, and dotted lines when neither is significant. Transparent ribbons indicate 95% confidence intervals. Vertical grey lines indicate the long-term mean for the climate variable, shading indicates 1 SD.

Figure S14. Best GLS models for Scotty Creek (NW Territories, Canada)

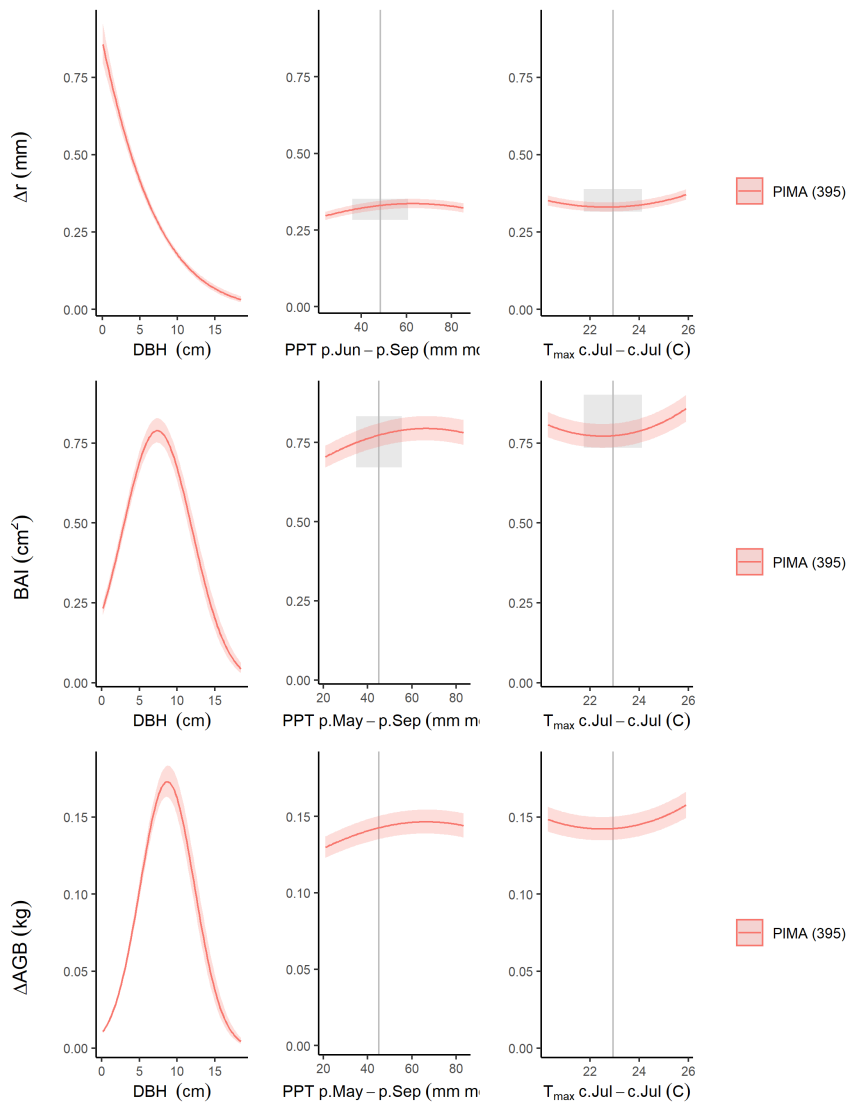


Figure S14 | Best GLS models for Scotty Creek (NW Territories, Canada) for all three growth metrics: Δr , BAI, and ΔAGB . Precipitation and temperature group variables are as selected by *climwin* (p=previous year, c=current year). For each species, relationships are plotted if included in top model, with best-fit polynomials plotted with solid lines when both first- and second-order terms are significant, dashed lines when only one term is significant, and dotted lines when neither is significant. Transparent ribbons indicate 95% confidence intervals. Vertical grey lines indicate the long-term mean for the climate variable, shading indicates 1 SD.

SI References

- Alfaro-Sánchez, R., Muller-Landau, H. C., Wright, S. J., & Camarero, J. J. (2017). Growth and reproduction respond differently to climate in three Neotropical tree species. *Oecologia*, 184(2), 531–541. doi:10.1007/s00442-017-3879-3
- Aus de Ar, R. (2018). Tree Rings of *Pinus ponderosa* and *Juniperus virginiana* Show Different Responses to Stand Density and Water Availability in the Nebraska Grasslands. *The American Midland Naturalist*, 180(1), 18. doi:10.1674/0003-0031-180.1.18
- Bumann, E., Awada, T., Wardlow, B., Hayes, M., Okalebo, J., Helzer, C., ... Cherubini, P. (2019). Assessing responses of *Betula papyrifera* to climate variability in a remnant population along the Niobrara River Valley in Nebraska, U.S.A., Through dendroecological and remote-sensing techniques. *Canadian Journal of Forest Research*, 49(5), 423–433. doi:10.1139/cjfr-2018-0206
- Helcoski, R., Tepley, A. J., Pederson, N., McGarvey, J. C., Meakem, V., Herrmann, V., ... Anderson-Teixeira, K. J. (2019). Growing season moisture drives interannual variation in woody productivity of a temperate deciduous forest. *New Phytologist*, 223(3), 1204–1216. doi:10.1111/nph.15906
- Kašpar, K., Tumajer, J., Vašíčková, I., & Šamonil, P. (n.d.). Species-specific climate-growth interactions determine the future tree species dynamics of the mixed Central European mountain forests.
- Maxwell, J. T., Harley, G. L., & Robeson, S. M. (2016). On the declining relationship between tree growth and climate in the Midwest United States: The fading drought signal. *Climatic Change*, 138(1-2), 127–142. doi:10.1007/s10584-016-1720-3
- Sniderhan, A. E., & Baltzer, J. L. (2016). Growth dynamics of black spruce (*Picea mariana*) in a rapidly thawing discontinuous permafrost peatland: Growth Dynamics Boreal Peatlands. *Journal of Geophysical Research: Biogeosciences*, 121(12), 2988–3000. doi:10.1002/2016JG003528
- Tumajer, J., Altman, J., Štěpánek, P., Treml, V., Doležal, J., & Cienciala, E. (2017). Increasing moisture limitation of Norway spruce in Central Europe revealed by forward modelling of tree growth in tree-ring network. *Agricultural and Forest Meteorology*, 247, 56–64. doi:10.1016/j.agrformet.2017.07.015
- Vlam, M., Baker, P. J., Bunyavejchewin, S., & Zuidema, P. A. (2014). Temperature and rainfall strongly drive temporal growth variation in Asian tropical forest trees. *Oecologia*, 174(4), 1449–1461. doi:10.1007/s00442-013-2846-x